[3] Love, A. E. H., *A Treatise on the Mathematical Theory of Elasticity* (Cambridge University Press, New York, 1927), 4th ed., pp. 496–498.

[4] Tranter, C. J., *Integral Transforms in Mathematical Physics* (Methuen and Co., London, 1959), 2nd ed., pp. 88–90.

Hypersonic Flow Visualization Using Tufts of Pure Carbon Yarn

H. Harvey Album*
Stanford University, Palo Alto, Calif.

In hypersonic wind-tunnel experiments, tufts can be useful in a host of problems including visual assessment of spanwise flows in boundary layers on yawed and unyawed plane bodies, cross flows on pitched axisymmetric bodies, sting interference, open and closed wakes, and separated-reattaching flows. Tufts of wool, cotton, and similar organic materials have been used for some time in subsonic and in supersonic wind-tunnel experiments. However, the high temperatures associated with many hypersonic wind tunnels often have precluded the use of this simple yet extremely valuable technique. The purpose of this note is to suggest the use of tufts made of pure carbon yarn for high-temperature hypersonic wind-tunnel experiments.

Carbon tufts were used in hypersonic experiments at the Hypersonic Research Laboratory of the Aerospace Research Laboratories (U. S. Air Force) for flow visualization of hypersonic flows. These tufts exhibited many of the characteristics of wool. They were small and flexible, but they also had sufficient strength and temperature durability to withstand high temperatures associated with hypersonic tunnel flow conditions. Although a complete study of the characteristics and limitations of carbon yarn tufts has not been made, the following example should serve to demonstrate this point. The pictures in Fig. 1 show pure carbon yarn tufts, which were used on an axisymmetric model in a flow with a Mach number of about 14, a stagnation temperature of 2100° R, and a stagnation pressure of 1000 psia. The model's surface temperature was about 1300°R. The maximum model diameter is 0.75 in. In this case, the tufts were attached to the model with a very small amount of Pliobond (a suggestion of W. D. Humphries of Systems Research Corporation). The tufts shown contain as many as 50 strands. Tufts of from 2 to 5 strands also have been used with success under the same conditions, but photographs of these tufts were not suitable for reproduction. Tufts made of quartz fibers, Pyrex fibers, and a half-mil wire also were tried under similar conditions, but they were either too stiff or were attracted to the model's surface.

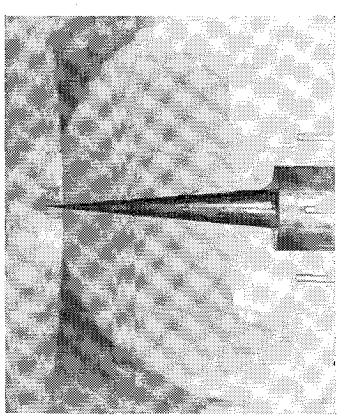

Fig. 1 Carbon yarn tufts in hypersonic separation experiment, Mach number 14, stagnation temperature 2100°R.

Questions as to the effects of these tufts on the flow field and the size and flexibility required to show the flow directions remain open. These are factors that depend upon each case being considered just as in lower speed flows. However, carbon yarn tufts are commercially available in a form that allows the experimentalist a wide latitude in selecting tuft lengths and thicknesses.

Received April 6, 1965.

* Graduate Student, Air Force Institute of Technology Program, Thermosciences Division, Mechanical Engineering Department; also Captain, U. S. Air Force. Member AIAA.

Optimum Hypersonic Lifting Surfaces Close to Flat Plates

J. D. Cole* and J. Aroesty†
The Rand Corporation, Santa Monica, Calif.

Nomenclature

θ = wedge angle
$\tilde{p}_2$ = undisturbed wedge pressure
p' = dimensionless pressure perturbation
p_2 = $\tilde{p}_2(1 + p')$
M_2 = Mach number along unperturbed wedge
λ = reflection coefficient
k = $1 - [\tan\bar{\beta}/(M_2^2 - 1)^{1/2}]/1 + [\tan\bar{\beta}/(M_2^2 - 1)^{1/2}]$ = relative abscissa of wave and its reflection
$\bar{\beta}$ = angle between undisturbed shock wave and wedge
x = distance from apex along unperturbed wedge
γ = ratio of specific heats
Y_x = dimensional perturbation normal to original wedge surface

Studies of hypersonic lifting vehicles have led us to the investigation of two-dimensional lifting surfaces possessing maximum lift-to-drag ratio for fixed lift in the limit of inviscid hypersonic flow. Earlier work on this problem utilized hypersonic Newtonian theory to obtain two key results; the application of the slender-body version of Newtonian theory to the class of two-dimensional power law surfaces indicated that the flat plate is the optimum such surface in terms of $(C_L/C_D)_{\max}$ for fixed C_L, and the application of the full Newtonian-Busemann theory indicated that the optimum wing is a flat plate fitted with a narrow "Newtonian chine strip" at its trailing edge.[1]

Our approach to this problem is to consider the lower surface of a lifting airfoil, which is close to a flat plate in shape. By restricting our analysis to such shapes, we are able to use the first-order pressure correction caused by the perturbation of a wedge profile in supersonic flow, as given by Chernyi.[2]

The formula given by Chernyi (Ref. 2, p. 186), and quoted in this paper, stems from a first-order solution of the full equations of motion for supersonic flow of a perfect gas past a slightly perturbed wedge at arbitrary Mach number and wedge angle (Fig. 1).

The first-order pressure perturbation caused by the slight perturbation of a wedge profile in supersonic flow is

$$\tilde{p}_2 p'(x) = \frac{\gamma M_2^2 \tilde{p}_2}{(M_2^2 - 1)^{1/2}} \left[Y'(x) + 2 \sum_{n=1}^{\infty} \lambda^n Y'(k^n x) \right] \quad (1)$$

Received March 29, 1965. Any views expressed in this paper are those of the authors. They should not be interpreted as reflecting the views of the Rand Corporation or the official opinion or policy of any of its governmental or private research sponsors. Papers are reproduced by the Rand Corporation as a courtesy to members of its staff.

* Consultant; also Professor, California Institute of Technology.
† Engineer. Member AIAA.

The lift of this slightly perturbed wedge is given by

$$L = \int_0^l p_2 \cos[\theta + Y'(x)]dx \tag{2}$$

and the drag may be calculated from

$$D = \int_0^l p_2 \sin[\theta + Y'(x)]dx \tag{3}$$

where l is the unperturbed wedge length. Linearizing, performing the integrations, and fixing the unperturbed wedge angle θ by setting $Y(0) = Y(l) = 0$, we obtain for lift and drag:

$$L = \tilde{p}_2 l \left\{\cos\theta \left[1 + \frac{2\gamma M_2^2}{(M_2^2 - 1)^{1/2}} \sum_{n=1}^{\infty} \left(\frac{\lambda}{k}\right)^n Y(k^n)\right]\right\} \tag{4a}$$

$$D = \tilde{p}_2 l \left\{\sin\theta \left[1 + \frac{2\gamma M_2^2}{(M_2^2 - 1)^{1/2}} \sum_{n=1}^{\infty} \left(\frac{\lambda}{k}\right)^n Y(k^n)\right]\right\} \tag{4b}$$

The equation in Ref. 2 (p. 187) corresponding to Eq. (4b) omits the factor $(1/k)^n$ under the summation sign. For small wedge angles θ, application of the hypersonic limits $M_\infty \to \infty$, $M_\infty\theta \to \infty$ yields

$$C_L \equiv \frac{L}{ql} \equiv \frac{L}{(\gamma/2)p_\infty M_\infty{}^2 l} = (\gamma + 1)\theta^2 \left\{1 + \frac{2}{\theta}\left(\frac{2\gamma}{\gamma - 1}\right)^{1/2} \times \sum_{n=1}^{\infty} \left(\frac{\lambda_\infty}{k_\infty}\right)^n Y(k_\infty{}^n)\right\} \tag{5a}$$

$$C_D \equiv \frac{D}{ql} = (\gamma + 1)\theta^3 \left\{1 + \frac{2}{\theta}\left(\frac{2\gamma}{\gamma - 1}\right)^{1/2} \sum_{n=1}^{\infty} \left(\frac{\lambda_\infty}{k_\infty}\right)^n \times Y(k_\infty{}^n)\right\} \tag{5b}$$

where

$$\lambda_\infty = \frac{1 - \left(\frac{\gamma_\infty}{2(\gamma - 1)}\right)^{1/2}}{1 + \left(\frac{\gamma}{2(\gamma - 1)}\right)^{1/2}} = -\frac{1 - \left(2\frac{\gamma - 1}{\gamma}\right)^{1/2}}{1 + \left(2\frac{\gamma - 1}{\gamma}\right)^{1/2}} \tag{6a}$$

and

$$k_\infty = 1 - \left(\frac{\gamma - 1}{2\gamma}\right)^{1/2} \Big/ 1 + \left(\frac{\gamma - 1}{2\gamma}\right)^{1/2} \tag{6b}$$

We also note that $|\lambda_\infty/k_\infty| < 1$. Since $Y(k_\infty{}^n)$ is the perturbation to the wedge profile at the fraction $k_\infty{}^n$ of the chord length, a suitable inequality condition for the validity of the previous analysis is $|Y(k_\infty{}^n)| < \epsilon k_\infty{}^n\theta$, where ϵ is a small number, say 0.1. This constraint limits the maximum perturbation in the profile to a fixed fraction ϵ of the original coordinate and, for smooth shapes, implies a bound on the maximum perturbation in the slope. For fixed C_L, the lift-to-drag ratio is

$$\frac{C_L}{C_D} = \left[\frac{C_L}{\gamma + 1}\right]^{-1/2} \left[1 + \left(\frac{2\gamma}{\gamma - 1}\right)^{1/2} \sum_{n=1}^{\infty} \left(\frac{\lambda_\infty}{k_\infty}\right)^n \times \frac{Y(k_\infty{}^n)}{\theta} + \ldots\right] \tag{7}$$

The maximum value of C_L/C_D is obtained thus when

$$\sum_{n=1}^{\infty} \left(\frac{\lambda_\infty}{k_\infty}\right)^n \frac{Y(k_\infty{}^n)}{\theta}$$

is a maximum. Using the inequality condition, we obtain

$$\left(\frac{C_L}{C_D}\right)_{\max} = \left(\frac{C_L}{\gamma + 1}\right)^{-1/2} \left[1 + \left(\frac{2\gamma}{\gamma - 1}\right)^{1/2} \epsilon \frac{|\lambda_\infty|}{1 - |\lambda_\infty|}\right] \tag{8a}$$

where we have set

$$Y(k_\infty{}^n) = (-1)^n \epsilon k_\infty{}^n \theta \tag{8b}$$

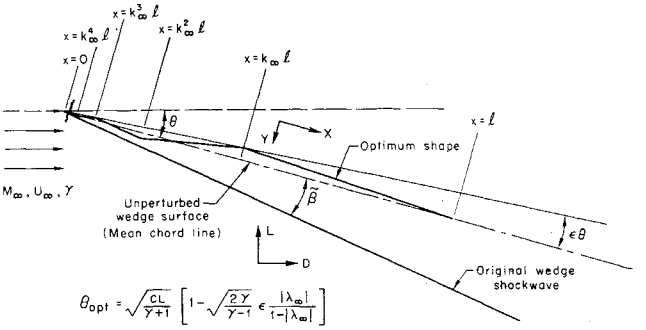

Fig. 1 Optimum lifting surface for fixed perturbation ϵ of a flat plate.

and used the identity

$$(1 - |\lambda_\infty|)^{-1} = 1 + |\lambda_\infty| + |\lambda_\infty|^2 + |\lambda_\infty|^3 + |\lambda_\infty| + \ldots \qquad \text{if } |\lambda_\infty| < 1$$

The maximum perturbation in slope for this shape is $\epsilon(1 + k)/1 - k$ (Fig. 1).

Introducing an inclined flat plate with the same C_L as a standard for comparison, we obtain

$$\left[\frac{(C_L/C_D)_{\max}}{C_L/C_D)_{\text{plate}}}\right] - 1 = \left(\frac{2\gamma}{\gamma - 1}\right)^{1/2} \epsilon \frac{|\lambda_\infty|}{1 - |\lambda_\infty|} \tag{9}$$

The angle of attack of the mean chord line, referred to as the angle of attack of the reference flat plate, is

$$\frac{\theta_{\text{opt}}}{\theta_{\text{plate}}} = 1 - \left(\frac{2\gamma}{\gamma - 1}\right)^{1/2} \frac{|\lambda_\infty|}{1 - |\lambda_\infty|} \epsilon \tag{10}$$

The pressure distribution, when referred to the pressure on the inclined plate with equal C_L, is

$$\frac{p_{\text{opt}}}{p_{\text{plate}}} - 1 = \epsilon \left(\frac{2\gamma}{\gamma - 1}\right)^{1/2} \left\{\frac{k}{1 - k}\right\} \left\{\frac{|\lambda_\infty|4}{1 - |\lambda_\infty|}\right\} \tag{11a}$$

for $k < x/l < 1$ and

$$\frac{p_{\text{opt}}}{p_{\text{plate}}} - 1 = \epsilon \left(\frac{2\gamma}{\gamma - 1}\right)^{1/2} \left\{(-1)^N \left[1 + \frac{2|\lambda_\infty|}{1 - |\lambda_\infty|}\right] \times \frac{1 + k}{1 - k} - 2\frac{2|\lambda_\infty|}{1 - |\lambda_\infty|}\right\} \tag{11b}$$

for $k^{N+1} < x/l < k^N$ when $N = 1, 2, 3, \ldots$.

Although it is true that a proper optimization has not been performed because of the indefiniteness of the perturbation parameter ϵ, these results still imply that it is possible to design two-dimensional concave hypersonic lifting surfaces, which, in the absence of viscous effects, are superior to flat plates by virtue of favorable interference effects. For example, a simple flapped surface (Fig. 2), which consists of two flat plates, intersecting at a distance $\epsilon kl\theta$ above the mean chord line at the kth fraction of the chord length, yields almost the same improvement as the surface considered

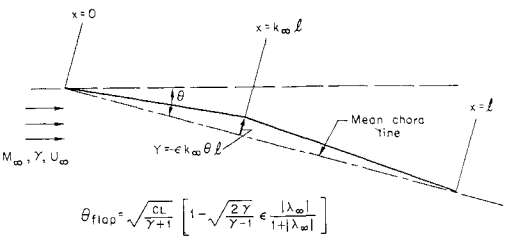

Fig. 2 Simple flapped surface, which is superior to flat plate.

previously which has an infinite number of changes in slope; i.e.,

$$\frac{(C_L/C_D)_{\text{flap}}}{(C_L/C_D)_{\text{plate}}} - 1 = \epsilon \left(\frac{2\gamma}{\gamma - 1}\right)^{1/2} \frac{|\lambda_\infty|}{1 + |\lambda_\infty|} \qquad (12)$$

References

[1] Hayes, W. and Probstein, R., *Hypersonic Flow Theory* (Academic Press Inc., New York, 1959).

[2] Chernyi, G., *Introduction to Hypersonic Flow* (Academic Press Inc., New York, 1961).

High-Temperature Kinetics of Graphite Oxidation by Dissociated Oxygen

DANIEL E. ROSNER* AND H. DONALD ALLENDORF†
AeroChem Research Laboratories,‡ Inc., Princeton, N.J.

Introduction

THE need to predict graphite and charring plastic ablation heat-shield behavior for atmospheric entry vehicles has motivated a great deal of recent research on the oxidation rate of graphite.[1–8] Based on this work a generally accepted overall picture has emerged (cf., Fig. 1) in which one distinguishes three fundamentally different regimes: 1) chemically controlled heterogeneous oxidation, 2) diffusion controlled heterogeneous oxidation, and 3) a sublimation regime in which the carbon oxidation reactions are "forced off" the surface. Among the assumptions that have been used to analyze the position and structure of the transition from chemically controlled to diffusion controlled heterogeneous oxidation two seem particularly suspect, namely, 1) the assumption that the specific reactivity of graphite has a simple Arrhenius behavior, and 2) the assumption that oxygen atoms play no role in the kinetics of graphite oxidation. As will be seen, these assumptions are not justifiable, and the effects of relaxing them are especially large for the case of lifting re-entry from earth orbit.

This situation can be anticipated on the following grounds. Several calculations (e.g., those of Ref. 7) based on the preceding assumptions reveal that a substantial portion of the re-entry trajectory of such vehicles takes place in this so-called "intermediate" kinetic-diffusion regime. Early entry into the diffusion-controlled regime is predicted[7] only using an unrealistic upper limit for the reactivity of commercial graphite in O_2 environments, a fact that can be verified by noting that the oxidation probability§ ϵ, corresponding to these "fast" kinetics, exceeds unity at surface temperatures above ~1200°K. In reality, of course, ϵ cannot exceed a number of order unity, and hence, simple Arrhenius behavior does not extend to these temperatures.¶ The assumption that O atoms, if present, should play no role in the kinetics[8] runs counter to existing experimental data for this[9] and similar[10–14] surface reactions. Actually, for radiation-cooled lifting re-entry vehicles, one expects nonequilibrium concentrations of O atoms at the gas/solid interface, since oxygen atom recombination in the boundary layer is negligible owing both to the low-density levels and high surface temperatures.[15–17] For these reasons, we have initiated studies of the true kinetics of the high-temperature oxidation of graphite and related refractory materials by oxygen atoms and oxygen molecules in the same apparatus. Some preliminary experimental results for graphite and their implications for ablation analyses are discussed below.

Experimental

The techniques used to study the true kinetics of graphite attack by both O atoms and O_2 are similar to those used in our previous studies of the molybdenum and tungsten reactions.[11–13] Briefly, our apparatus consists of a part Vycor-part Pyrex vacuum flow system coupled to a 25 liter/sec mechanical pump. Metered argon/O_2 mixtures are passed through a 2450 Mc/sec, 125-w microwave discharge cavity, downstream of which the gas encounters an electrically heated graphite filament fed by a regulated dc power supply. Simultaneous with a current measurement, the voltage drop across the central 0.55 cm of the filament is monitored using spring loaded contacts leading to a recording potentiometer. During an experiment the filament is maintained at constant temperature by altering the current in accord with an optical pyrometer output, thereby allowing the decrease in filament diameter caused by the reaction to be related to the increase in electrical resistance. The absolute value of the surface temperature is determined from the pyrometer reading, as corrected using the emittance-temperature relation for the specimen.[18] O atom concentrations in the vicinity of the filament are obtained using the NO_2 light titration technique.[19] The data reported here were obtained using commercially available 20-mil-diam graphite rods.** In all cases, external diffusion as well as thermal accommodation limitations were ruled out on the basis of the absence of flow rate and carrier gas effects on the observed reaction rates. This invariance of the observed reaction rates under changes in aerodynamic parameters is not unexpected under the present experimental conditions, which corresponded to a Knudsen number of about $\frac{1}{10}$, a Reynolds number of about 10 (both based on gas properties of the approach flow, using filament diameter as the reference length), and Mach numbers up to 0.6.

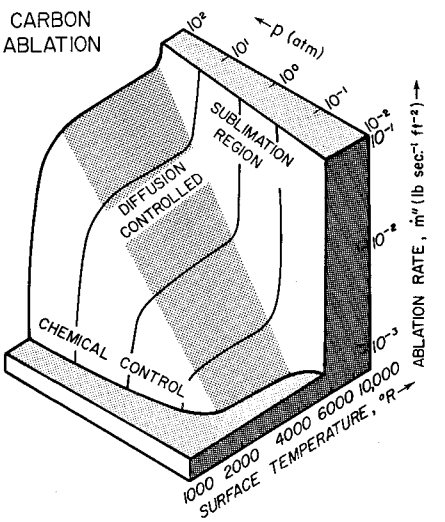

Fig. 1 Stagnation point ablation regimes for graphite in air (constructed from calculations reported in Refs. 2 and 6; nose radius = 1 ft).

Received November 30, 1964; revision received May 7, 1965. This work was supported by the Propulsion Division of the Office of Aerospace Research, U. S. Air Force Office of Scientific Research, under Contract No. AF 49(638) 1195, based on AeroChem TP-105 (November 20, 1964).

* Aeronautical Research Scientist. Associate Fellow Member AIAA.

† Chemical Engineer.

‡ Subsidiary of Pfaudler Permutit Inc.

§ This is defined, for example, as the fraction of O_2 collisions with the surface that lead to carbon atom removal from the lattice.

¶ Interestingly enough, if one fits all available lower temperature ($T_w < 1200$°K) $C(s) + O_2(g)$ data by the locally Arrhenius form $\epsilon = \epsilon_0 \exp(-E/RT)$, one finds that the pre-exponential factor ϵ_0 exceeds unity. Thus, simple high-temperature extrapolations of such data are inaccurate for the same reason.

** Electrographitic extruded rod, Grade 580, No. 710 V manufactured by the Speer Carbon Co., Pa.